VOL. 10, NO. 19, OCTOBER 2015 ISSN 1819-6608
ARPN Journal of Engineering and Applied Sciences

www.arpnjournals.com

A SUSCEPTIBILITY STUDY ON PIEZORESISTIVE SENSOR IN A PLIABLE AND RIGID ROBOTIC CLAWS MODEL

Abdulrahman Abdulkareem S. Al-Shanoon, Siti Anom Ahmad and Mohd. Khair B. Hassan
Department of Electrical and Electronics Engineering, Universiti Putra Malaysia, Selangor, Malaysia
E-Mail: abdulrahman89eng@gmail.com

ABSTRACT

This study has investigated and surveyed tactile pressure sensors, such as strain gauge, piezocapacitive, piezoelectric, piezoresistive, and pressure conductive rubber, according to robotic applications of these sensors. These tactile pressure sensors have been broadly used for robotic grasping operations. Moreover, through these tactile pressure sensors, the information on physical contacts and the external environment of robotic hand are reported and discovered. In this study, common piezoresistive pressure sensors (force-sensing resistor) have achieved favorable results in gripping an object; these results support that the piezoresistive technique is an appropriate approach for robotic implementations. Furthermore, two illustrative empirical findings have been performed using both rigid and pliable robotic claw surfaces. Experimental results have shown the correlation between input force and output voltage as well as the response of pressure sensor with different robotic claw resiliencies.

Keywords: robotics, piezoresistive, gripping manipulator, pliable and rigid surfaces, robotic claw resilience.

INTRODUCTION

People's daily activities could be achieved using the hand, which can execute difficult tasks at various angles and with high complexity. The human hand is created with tremendous structure and exact capability to maneuver motions and manipulate grasping tasks correctly [1–4]. However, the human hand still has some limitations to execute other tasks, such as dangerous or sophisticated operations in military and medical applications. In addition, errors have a high probability to occur in repetitive and maintenance tasks because the human hand is restricted by limited human ability.

Thus, in recent years, significant efforts have been devoted to improve robotic manipulators, such as robotic hand or robotic claw. Currently, robotic hands begin as indispensable, especially because robotic hands have been broadly implemented in significant applications [5], [6]. In addition, robotic hand is widely used in automotive manufacturing industries for functions such as picking and placing, sorting, packaging, and palletizing, as well as in assembly and material handling production lines that require human hand substitution [7–9].

The most important issue in robotic hand applications is that robotic hands require distributed tactile pressure sensors that enable robotic hands to recognize the external environment. The primary emphasis placed on tactile sensors widely used in robotic hand applications is to measure the physical interaction that occurs through the contact points between the pressure sensor and a subjected object. These tactile pressure sensors are designed and implemented based on different principle actions and materials, such as strain gauge, piezocapacitive, piezoelectric, pressure conductive rubber, and piezoresistive pressure sensors [10–14]. Researchers have focused on the comprehension of tactile sensor characteristics, and different useful illustrative applications have been performed in various fields in Refs. [15–17].

BACKGROUND STUDY

Robotic hand is considered a mechatronic instrument that can do some activities that are impossible for humans. Robotic hand is widely used in manufacturing and dangerous nuclear industries, as well as in precise applications such as military or medical implementations. In addition, repetitive and maintenance tasks could be achieved with high performance accuracy. Consequently, evolving robotic hand is required to cover a wide range of tasks and to provide robotic hand with special types of sensors that can measure the grasping force for a particular object. Grasping objects could be achieved using the dexterous robotic hand presented in Ref. [18], which is illustrated with the ability to grasp both soft and hard objects. In Refs. [19], [20], gripping operation has been implemented by robotic hands that use special types of tactile sensors, which employ physical properties and events through contact with objects. Many tactile sensors have been developed, and the sensor hardware has evolved to achieve certain gripping tasks. Moreover, to accomplish the gripping mechanism using robotic hand, some efforts have been expended in developing tactile pressure sensor structures, such as in Refs. [21], [22]. In most recent studies, advanced robotic manipulations have used tactile pressure sensors implemented in different applications. The main interesting issue in advanced robotic manipulation tasks is that robotic hand is required to be equipped with distributed tactile pressure sensors that can continuously provide information about the magnitude and direction of forces at all contact points between the sensing area and a subjected object. Numerous studies have reported the proposed method that uses tactile sensor information through physical contact between the sensor and an object to detect both pressure force and hardness of the object [23]. In addition, several studies have documented that tactile pressure sensors have been utilized successfully in different design concepts and action principles. These tactile sensors have presented the

process of determining physical features with the environment [24],[25], measuring applied forces exerted over an object and the art in tactile sensing and investigating trends [26–28].

Robotic hands have recently applied sensitive skin by using tactile pressure conductive rubber to perform a wide area of soft sensor skin that covers the whole body of robots. In addition, numerous authors have reported both analyses of trends using electrically conductive fabric and strings and conductive mechanism based on pressure sensitivity [29–33]. Furthermore, other devices have been designed to detect changes in resistance between a conductive rubber layer and have implemented contact electrodes [34].

An applied force to a piezoelectric material generates an electrical potential difference; this response is reversible. When the potential difference is supplied across two terminals of a piezoelectric material, the material strains. The piezoelectric phenomena could exist in "smart materials" with electrical crystalline structure. The generated voltage from a piezoelectric material can be calculated from the following equation: ($V = Sv \times P \times D$), where V is the voltage generated, Sv is the volt sensitivity of the material (volt × meters/Newton), P is the pressure (N/m2), and D is the thickness of the material (meters).

Strain gauge sensors exhibit a change in resistivity with strain. Strain gauges are frequently used in mechanical strain. Resistance increases when the material is stretched. One of the main obstacles is that strain gauge is highly susceptible to humidity and is very sensitive to temperature changes. Thus, Wheatstone bridge approaches are used to overcome this weakness. Although the mechanical nature of the strain gauge could not be recovered if the gauge is overloaded, the strain gauge can be used for a long time [35].

Capacitive tactile sensors comprise of two parallel plates, where a dielectric material is sandwiched. Capacitance can be expressed as $C = (A\varepsilon_0\varepsilon_r)/d$, where C is the capacitance, A is the overlapping area of the two plates, ε_0 is the permittivity of free space, ε_r is the relative permittivity of the dielectric material, and d is the distance between the two plates. The applied force changes the distance between the two plates; thereafter, electrical charges are generated [36], [37].

One of the well-known tactile pressure sensors is piezoresistive tactile pressure sensor, which has been widely used in robotic gripping implementations, such as gripping an object with different weights and shapes [38]–[41]. A key aspect of pressure sensor is the ability to indicate the touch situation or continuous pressure force that occurs between a subjected object and the pressure sensor. This indication occurs according to the change in sensor resistance corresponding with applied force. Thus, piezoresistive pressure sensor is considered an appropriate approach for gripping operations in robotic hands. The tactile pressure techniques that have been explained above are presented in Table-1. In Table-1, the merits and demerits of tactile pressure sensors are reviewed.

Table-1. Merits and demerits of different types of tactile pressure sensors [13].

Sensor type	Sensory modality	Merits	Demerits
Capacitive	Change in capacitance	I. Sensitive II. Low cost III. Availability of commercial A/D chips.	I. Cross-talk. II. Hysteresis. III. Complex Electronics.
Piezoresistive	Change in resistance	I. Sensitive II. Low Cost	I. high power consumption. II. Generally detect single contact point. III. Lack of contact force Measurement.
Piezoelectric	Strain stress (polarization)	I. Dynamic response. II. High bandwidth.	I. Temperature sensitive II. Not so robust electrical connection.
Strain gauge	Change in resistance	I. Sensing range sensitivity. II. Low cost. III. Established product.	I. Susceptible to temperature changes and humidity. II. Design complexity, non-linearity hysteresis.
Conductive rubber	Change in resistance	I. Physically flexible.	I. Mechanical hysteresis II. Non-linear response.

Pressure sensor structure and principle action

Force-sensing resistor (FSR) is a polymer thick film device that can indicate decrease in resistance with an increasing applied force to the active sensing area. The force sensitivity of FSR is appropriate for human touch control of electronic implementations. FSR is based on the piezoresistive sensing technology. FSR can be fabricated in different shapes and sizes to achieve sensing force purposes. Some features of this sensor, such as highly thin, linearity, low hysteresis and drift, and a wide range of temperature sensitivity, can be vital in providing accurate results in detection contact or continuous touch between two objects. Piezoresistive sensors can indicate changes in electrical resistance when mechanical stress is applied. Thus, this device is considered an appropriate approach for

robotic hands in gripping operations. In Ref. [42], the structure of pressure sensor comprises two layers of substrate; these layers contain printed semi-conductor components as the active area. As shown in Figure-1, the spacer adhesive layer is sandwiched between two substrate layers. The piezoresistance can be expressed as R in equation (1).

$$R = \frac{\rho \times l}{t \times \omega} \quad (1)$$

ρ = the resistivity,
l = length,
ω = width of the contact,
t = thickness of the piezoresistor

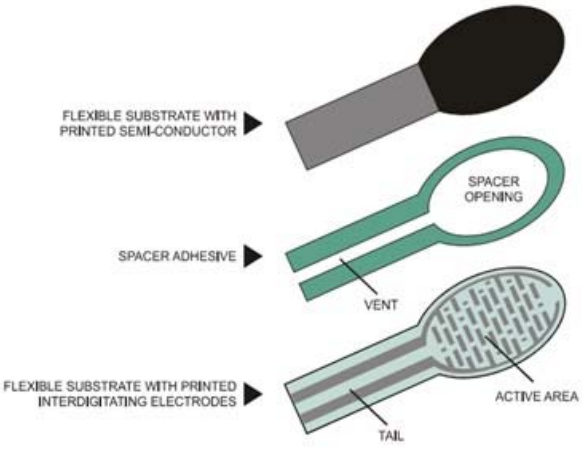

Figure-1. The construction of pressure sensor (FSR).

EXPERIMENTAL SETUP

Schematic diagram of the pressure sensor

To integrate the FSR sensor into an application, force-to-voltage circuit can be implemented to incorporate the output voltage with input force. Calibration is the approach to express the output into appropriate engineering units, such as Newton. The proposed circuit in this study is shown in Figure 2. This circuit is derived through a −5 V DC excitation voltage. An inverting operational amplifier (op-amp) has wired the pressure sensor with feedback reference resistance (RF). The purpose of supplying the pressure sensor with a negative input voltage is to ensure that high sensitivity occurs, and the pressure sensor output connects to the inverting input terminal of the op-amp to obtain a positive output voltage. The output voltage is changed based on the change in pressure sensor resistance. In addition, the pressure sensor sensitivity could be adjusted by both changing the RF and/or deriving the excitation voltage. The pressure sensor output voltage is expressed in equation (2).

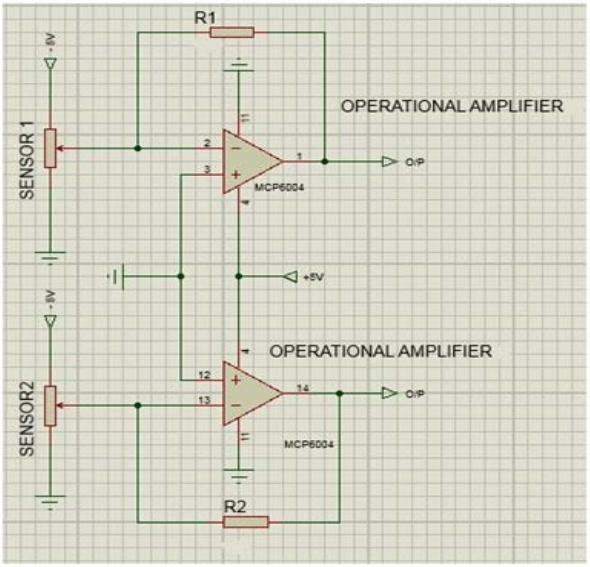

Figure-2. Schematic diagram of the proposed circuit.

$$V = -Vt \times Rf / Rs \quad (2)$$

V = the output voltage of the pressure sensor,
Vt = the D.C excitation input voltage,
Rf = feedback reference resistance,
Rs = pressure sensor resistance.

Pressure sensor conditioning and calibration

Gripping an object successfully and measuring the weight of the object is considered one of the main goals of this study. To achieve accurate output results from the pressure sensor, an essential step should be applied before calibrating and testing the sensor. This step is called exercising or conditioning the sensor, which helps diminish the effect of drift and hysteresis. The conditioning step is applied for new sensors and for sensors that have not been used for a long time. To perform this step, 110% of the maximum test weight is placed on the sensing area of the pressure sensor, and 5 s is needed to allow the sensor to stabilize the output resistance; this procedure is repeated 4 or 5 times. As shown in Figure-3, known calibration weights are used for the conditioning step. In this study, given that the calibration weights are larger than the sensing area, this step should use a puck. A puck is a piece of rigid material that is smaller than the sensing area of the pressure sensor. A puck helps ensure that the testing load path goes through the pressure sensor sensing area. Afterward, for calibration, 1/4 of the weight of the object is placed on the sensing area for about 5 s to obtain the best reading. The result is recorded, and the weight is removed. This procedure is repeated several times through the same process, but the weight of the object is increased gradually every single time until reaching the maximum weight. Finally, 6–7 sets of results have been recorded as curves on a graph. According to the principle action of the

pressure sensor, two curves can be obtained from the analog readout circuit. Resistance/conductance (1/R) versus force and voltage versus force. The correlation between the input force and the output voltage is proportional, whereas the correlation is inversely proportional between the input force and the output resistance. The output resistance decreases when the pressure force is increased on the pressure sensor sensing area, and the resistance is very high in case no load exists. The experimental results and discussion of these curves are illustrated in this study.

Figure-3. Experimental setup of pressure sensor.

Proposed robotic hand model

In this study, the proposed work focuses on designing and implementing a robotic hand model to grip an object with different weights. In Figure-4, this robotic hand model is featured with simple traits. The proposed robotic hand model is designed and implemented to accomplish the crucial aim of an object gripping that measures and calculates the response of the pressure sensor from contact points with the gripped object.

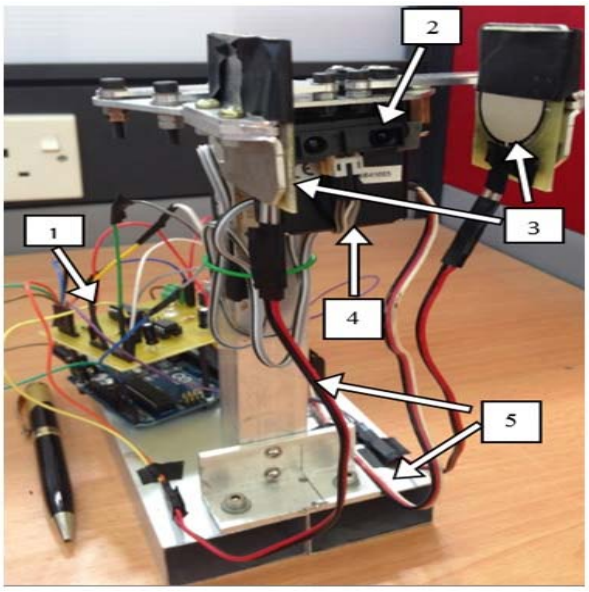

Figure-4. Proposed robotic hand model.

Where 1 denotes PCB, MCU, and power supply; 2 denotes IR sensor; 3 denotes pressure sensors; 4 denotes DC servo motor; and 5 denotes the proposed robotic hand structure.

A robotic hand has been designed and assembled in specific dimensions (100 mm × 205 mm × 215 mm). The robotic hand model consists of only one claw, and the maximum open dimension is 60 mm. This claw can be moved by using a DC servo motor within only one degree of freedom in the X-axis. The robotic hand can hold a weight of up to 3.187 N. In this study, a flat rectangular object is taken as a gripping sample. As shown in Figure-5, the weight and dimensions of this object are 0.4118 N and 84 mm × 130 mm, respectively. Definitely, the dimensions of the object should be larger than the claw of the robotic hand model to ensure that the object covers the entire sensing area of the pressure sensor attached to the claw.

Two piezoresistive pressure sensors (FSR) are used at both sides of the robotic claw to measure the continuous gripping force produced between the robotic hand and an object. This sensor works with diverse force ranges; with respect to the proposed design, the force range is 0–111 N. The sensing area of FSR is 25.4 mm in diameter, and the thickness is 0.203 mm. Furthermore, IR sensor is important in the motion of a robotic hand, given that IR is used to detect the existence of an object between the two robotic hand claws to provide the system with automatic robotic motion.

The selected microcontroller unit (MCU) is Arduino Uno R3. This MCU has been chosen with respect to the following purposes: analog-to-digital converter, motor driver, pulse width modulation signals, digital in/out pins, analog input pins, low cost, and excellent compatibility with external components. The integrated circuit that has been implemented in MCU is an ATmega328. Moreover, the PCB in this study has been designed and implemented utilizing electronic components with high-quality performance and low power cost. As shown in Figure-6, these circuits are used to obtain experimental works that grip an object safely.

Figure-5. Sample object for experiment.

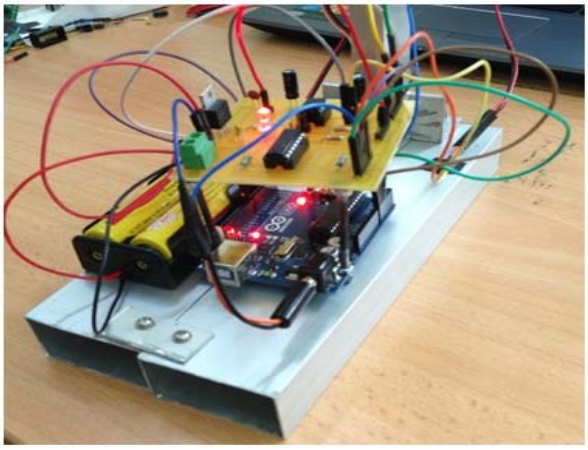

Figure-6. Printed circuit board and microcontroller are used for the experiment.

RESULTS AND DISCUSSION

The experimental results have reported the response of the pressure sensor resistance when the pressure force is changed. As shown in Figure-7, the graph presents the inverse correlation between the resistance in mega ohm and the pressure force in N. The resistance value is very high at no load case. This value decreases dramatically when the pressure force is 0.4118 N, and this point indicates that the object is gripped successfully. The resistance continuously decreases when the pressure force increases every step. Hence, the weight of the object increases gradually until reaching the full range of the proposed robotic hand ability. The conductance (1/R) curve is more linear than the resistance curve; thus, the conductance curve has been calculated for calibration and analysis. The linearity regression of the conductance curve is the inverse of the resistance curve, and this regression is important to calculate the residual of the curve. This residual value calculates the accuracy of the collected data.

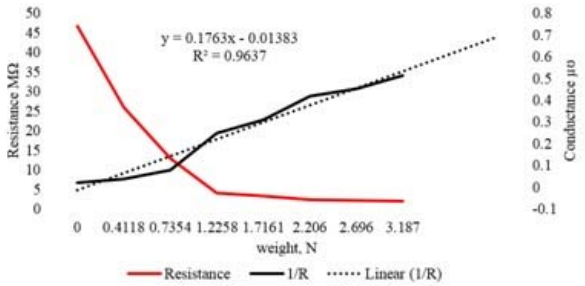

Figure-7. Resistance/conductance versus a series of weights.

In the first part of the experiment, as shown in Figure-4, pressure sensors have been attached on rigid robotic claws. The proportional correlation between the input pressure force (N) and the output volt (V) is presented in Figure-8. In this graph, each black point is considered an individual gripping task that grips the object with different weights. In the first gripping operation, the weight of the object is 0.4118 N, and the output voltage is 0.21 V. the resistance value dramatically decreases and reaches 25 megaohm approximately. After that, the weight gradually increases in each individual gripping operation until it covers the entire gripping ability. In this approach, the measured voltage of the pressure sensor continuous to increase and the resistance value decreases. The gripping operation procedures of the proposed robotic hand model are summarized as concise and comprehensible. After initializing the system, the robotic hand opens, and the prepared robotic fingers are moved to the initial position. Thereafter, the IR sensor monitors the distance sensing space between the fingers, and the DC servo motor commences to move when the IR sensor declares the inception point. The moment the proposed object touches the pressure sensors, the output signals are indicated through an analog readout circuit. This contact situation is recorded as the initial physical interaction. Thenceforth, the process can measure the pressure value and analyze the data to calculate the object weight that enables the control system to adjust the gripping force based on the estimated object weight.

In the second part of this experiment, the first part is repeated using a pliable robotic claw surface. In this study, as shown in Figure-9(a), the pliable surface is designed and implemented as a resilient surface. This pliable surface is called pillow and is mounted on the robotic claw, as shown in Figure-9(b). The pressure sensor is then attached to a pillow. Hence, the pressure sensor is sandwiched between the pillow and the object during the gripping operation. This pillow has been utilized for pressure sensor and object to ensure that the whole ability of the pressure sensor is already used and to prove that the rigid claw surface used in the first part of the experiment is the sensitive-enough surface in the proposed robotic hand model. As shown in Figure-10, the output voltage red line is reduced after the pressure force is increased to more than 2.206 N. This obvious regression curve indicates that the pressure sensor does not respond to the applied force, which is more than 2.206 N.

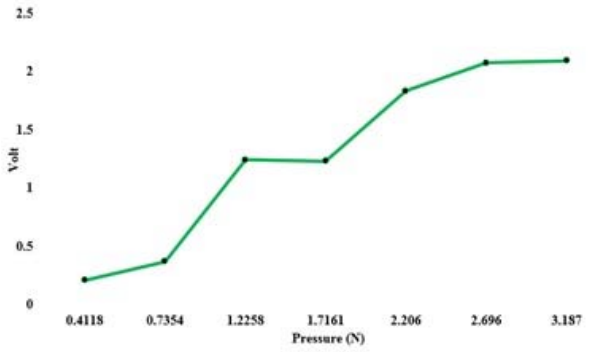

Figure-8. Output voltage over a series of weights before using pillows on the robotic hand claws model.

(a) Pillows

(b) Robotic claws with pillows

Figure-9. (a) The selected pillows for experiment, (b) the pillows have been attached on the claws of robotic hand model.

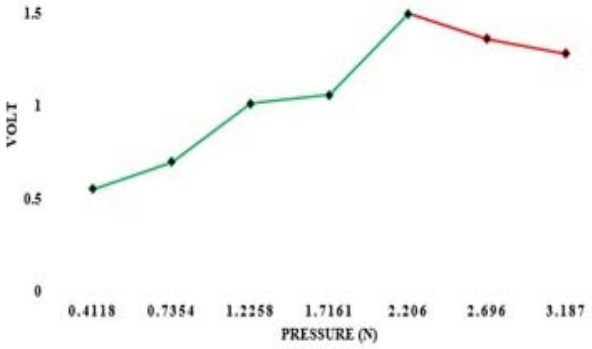

Figure-10. Output voltage regression curve over a series of weights after using pillows on the robotic hand claws model.

CONCLUSIONS

Various types of tactile pressure sensors are considered as appropriate techniques for robotic grasping tasks. These tactile sensors have been widely used according to the robotic fields of the sensors, such as strain gauge, piezocapacitive, piezoelectric, piezoresistive, and pressure conductive rubber. This study illustrates practically that piezoresistive pressure sensor is effective for gripping applications. In addition, the gripping mission investigates both pliable and rigid robotic claw model surface. The experimental results are emphasized in the second part of the experiment. In Figure-11, the residual value (R^2 = 0.9253) calculated from the linearity data of the first part of the experiment is better than the second residual value ($S{\cdot}R^2$ = 0.7756) calculated from the second part of the experiment. For calculation and analysis, the first R^2 is more acceptable than the second $S{\cdot}R^2$; thus a slight change occurs between R^2 and $S{\cdot}R^2$ of around 0.1497, which is inadmissible for calculation and analytical purposes. Basically, R^2 indicates how accurate the measured voltage is. Table-2 shows the experimental results between the first and second parts of the experiment.

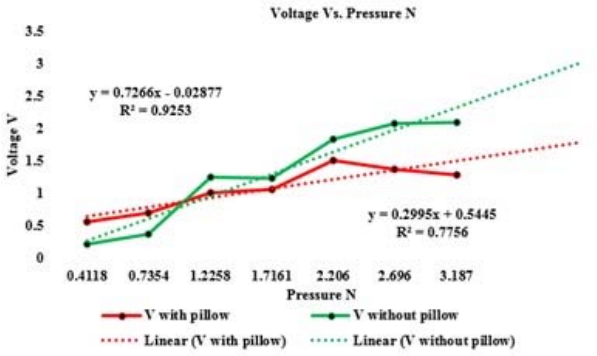

Figure-11. Output voltage over a series of weights for both robotic claws with pillows and without pillows.

Table-2. Experimental results between the two methods based on the proposed robotic hand model.

	Rigid surface without pillows	Pliable surface with pillows
R^2, S.R^2:Residual	0.9253	0.7756
Force range	0.4118 up to 3.187 N	0.4118 up to 2.206 N
Max. o/p volt	2.093 V	1.4985 V
$R^2 - S.R^2$	0.1497	

REFERENCES

[1] J. lee Kunii and T. L. 1995. "Model-based Analysis of Hand Posture. IEEE Comput. Graph. Appl., Vol. 15, No. 5, pp. 77–86.

[2] Y. Koike 1992. Human Hand Stiffness During Discrete Point-to-point Multi-joint Movement. Proc. Annu. Int. Conf. IEEE Eng. Med. Biol. Soc., pp. 1628–1629.

[3] R. S. Johansson and A. B. Vallbo. 1970. Tactile Sensibility In The Human Hand: Relative And Absolute Densities Of Four Types Of

Mechanoreceptive Units In Glabrous Skin. J. Physiol., Vol. 286, pp. 283–300.

[4] J. Lin, Y. Wu and T. Huang 2002. Capturing human hand motion in image sequences. Proc. Work. Motion Video Comput., pp. 99 – 104.

[5] P. Lin, G. Bekey and K. Abney. 2008. Autonomous military robotics: Risk, ethics, and design. Cal. Poly. Stat. Univer., San Luis, pp. 4–112.

[6] S. P. Dharia and T. Falcone. 2005. Robotics in reproductive medicine. Fertil. Steril., Vol. 84, No. 1, pp. 1–11.

[7] A. Blomdell and I. Dressler. 2010. Flexible application development and high-performance motion control based on external sensing and reconfiguration of ABB industrial robot controllers. IEEE Int. Conf. Robot. Autom., pp. 62–66.

[8] T. Brogårdh. 2007. Present and future robot control development—An industrial perspective. Annu. Rev. Control, Vol. 31, No. 1, pp. 69–79.

[9] Z. Pan, J. Polden, N. Larkin, S. Van Duin and J. Norrish. 2012. Recent progress on programming methods for industrial robots. Robot. Comput. Integr. Manuf., Vol. 28, No. 2, pp. 87–94.

[10] M. Lee and H. Nicholls. 1999. Tactile sensing for mechatronics—a state of the art survey Mechatronics, Vol. 9, No. 1, pp. 1–31.

[11] R. S. Dahiya, G. Metta, M. Valle, and G. Sandini (2010). Tactile Sensing—From Humans to Humanoids. IEEE Trans. Robot., Vol. 26, No. 1, pp. 1–20.

[12] M. E. Eltaib and J. Hewit. 2003. Tactile sensing technology for minimal access surgery—a review. Mechatronics, Vol. 13, No. 10, pp. 1163–1177.

[13] R. Dahiya and M. Valle. 2008. Tactile sensing for robotic applications," in Sensors, Focus on Tactile, Force and Stress Sensors, no. December, 2008, pp. 289–304.

[14] K. nori Shida and J. Yuji. 1996. Discrimination of Material Property by Pressure-Conductive Rubber Sheet Sensor with Multi-Sensing Function," Ind. Electron. ISIE '96., Proc. IEEE Int. Symp., Vol. 1, pp. 54–59.

[15] J. Dargahi and S. Najarian. 2005. Advances in tactile sensors design/manufacturing and its impact on robotics applications – a review. Ind. Robot An Int. J., Vol. 32, No. 3, pp. 268–281.

[16] M. R. Cutkosky, R. D. Howe and W. R. Provancher. 2008. Force and Tactile sensors. Springer Handb. Robot., pp. 455–476.

[17] R. Tajima, S. Kagami, M. Inaba and H. Inoue. 2002. Development of soft and distributed tactile sensors and the application to a humanoid robot," Adv. Robot., Vol. 16, No. 4, pp. 381–397.

[18] J. Alcazar and L. Barajas. 2010. Dexterous robotic hand grasping method for automotive parts. Humanoid Robot. (Humanoids), 10th IEEE-RAS Int. Conf., pp. 282–287.

[19] D. Goeger, N. Ecker and H. Woern. 2009. Tactile sensor and algorithm to detect slip in robot grasping processes. IEEE Int. Conf. Robot. Biomimetics, pp. 1480–1485.

[20] H. Yousef, M. Boukallel and K. Althoefer. 2011. Tactile sensing for dexterous in-hand manipulation in robotics—A review," Sensors Actuators A Phys., Vol. 167, No. 2, pp. 171–187.

[21] B. Choi and H. R. Choi. 2005. Development of tactile sensor for detecting contact force and slip. IEEE/RSJ Int. Conf. Intell. Robot. Syst., pp. 1977–1982.

[22] M. Shimojo, A. Namiki, M. Ishikawa, R. Makino and K. Mabuchi. 2004. A Tactile Sensor Sheet Using Pressure Conductive Rubber With Electrical-Wires Stitched Method. IEEE Sensors Journal, Vol. 4, No.5, pp. 589–596.

[23] M. Shikida, T. Shimizu, K. Sato and K. Itoigawa. 2003. Active tactile sensor for detecting contact force and hardness of an object," Sensors Actuators A Phys., Vol. 103, No. 1–2, pp. 213–218.

[24] R. De Souza and K. Wise. 1997. A very high density bulk micromachined capacitive tactile imager. Proc. Int. Solid State Sensors Actuators Conf. (Transducers '97), pp. 1473–1476.

[25] H. Takizawa, H. Tosaka, R. Ohta, S. Kaneko and Y. Ueda. 1999. Development of a microfine active bending catheter equipped with MIF tactile sensors. Tech. Dig. IEEE Int. MEMS 99 Conf. Twelfth IEEE Int. Conf. Micro Electro Mech. Syst. (Cat. No.99CH36291), pp. 412–417.

[26] P. Allen, A. Miller, P. Oh and B. Leibowitz. 1999. Integration of vision, force and tactile sensing for grasping. Int. J. Intell. Mach., Vol. 4, pp. 129–149.

[27] T. Yoshikawa. 1996. Hybrid position/force control of flexible-macro/rigid-micro manipulator systems. IEEE Trans. Robot. Autom., Vol. 12, No. 4, pp. 633–640.

[28] I. Payo, V. Feliu, and O. D. Cortázar. 2009. Force control of a very lightweight single-link flexible arm based on coupling torque feedback," Mechatronics, Vol. 19, No. 3, pp. 334–347.

[29] Y. Huang, B. Xiang and X. Ming. 2008. Conductive mechanism research based on pressure-sensitive conductive composite material for flexible tactile sensing. Proc. IEEE Int. Conf. Inf. Autom. ICIA, pp. 1614–1619.

[30] M. Inaba and Y. Hoshino. 1996. A full-body tactile sensor suit using electrically conductive fabric and strings. Proc. IEEE/RSJ Int. Conf. Intell. Robot. Syst. IROS '96, Vol. 2, pp. 450–457.

[31] S. Teshigawara and K. Tadakuma. 2009. High Speed and High Sensitivity Slip Sensor Utilizing Characteristics of Conductive Rubber. J. Robot. Mechatronics, Vol. 21, No. 2, pp. 200–208.

[32] S. Teshigawara, T. Tsutsumi, S. Shimizu, Y. Suzuki, A. Ming, M. Ishikawa, and M. Shimojo 2011. Highly sensitive sensor for detection of initial slip and its application in a multi-fingered robot hand. IEEE Int. Conf. Robot. Autom., pp. 1097–1102.

[33] S. Teshigawara, K. Tadakuma, M. Ishikawa and M. Shimojo. 2010. High sensitivity initial slip sensor for dexterous grasp. IEEE Int. Conf. Robot. Autom, pp. 4867–4872.

[34] W. Hillis. 1982. A high-resolution imaging touch sensor. Int. J. Rob. Res., Vol. 1, No. 2, pp. 33–44.

[35] D. Stefanescu. 2011. Strain gauges and Wheatstone bridges—Basic instrumentation and new applications for electrical measurement of non-electrical quantities. Syst. Signals Devices (SSD), 8th Int. Multi-Conference, pp. 1 – 5.

[36] M. I. Tiwana, S. J. Redmond and N. H. Lovell. 2012. A review of tactile sensing technologies with applications in biomedical engineering. Sensors Actuators A Phys., Vol. 179, pp. 17–31.

[37] K. Arshak, D. Morris, O. Korostynska and E. Jafer. (2004). Novel silicone-based capacitive pressure sensors with high sensitivity for biomedical applications. e-Polymers Collab. with Upcom. Glob. Conf. Polym. Compos. Mater., Vol. 4, No. 1, pp. 684–694.

[38] A. S. Fiorillo. 1997. A piezoresistive tactile sensor. IEEE Trans. Instrum. Meas., Vol. 46, No. 1, pp. 15–17.

[39] A. M. M. Almassri, W. Z. W. Hasan, S. a. Ahmad, and A. J. Ishak. 2013. A sensitivity study of piezoresistive pressure sensor for robotic hand. RSM IEEE Reg. Symp. Micro Nanoelectron., pp. 394–397.

[40] T. Lomas, A. Tuantranont and F. Cheevasuvit. 2003. Micromachined Piezoresistive Tactile Sensor Array Fabricated By Bulk-Etched Mumps Process. Circuits Syst.. ISCAS '03. Proc. Int. Symp., Vol. 4, pp. 856–859.

[41] A. Wisitsoraat, V. Patthanasetakul, T. Lomas and A. Tuantranont. 2007. Low cost thin film based piezoresistive MEMS tactile sensor. Sensors Actuators A Phys., Vol. 139, No. 1–2, pp. 17–22.

[42] I. Electronics. 2007. Interlink Electronics Inc., FSR integration Guide and Evaluation parts catalog with suggested Electrical interfaces. Version 1.0, 90-45632 Rev. D,. [Online]. Available: http://www.interlinkelectronics.com/. [Accessed: 27-Mar-2015].